

---

1 Article

2 **Three-Dimensional Physical Model Test Study on**  
3 **Mining-Induced Strata Movement of Open-Pit Final**  
4 **Slope**

5 **Kunpeng Gao<sup>1</sup>, Guoxiang Yang<sup>1,\*</sup> and Nengxiong Xu<sup>1</sup>**

6 <sup>1</sup> School of engineering and technology, China University of Geosciences, 100083, Beijing, PRC

7 \* Correspondence: yanggx@cugb.edu.cn; Tel.: +86-10-8232-2627

8 **Abstract:** Strata and surface movement induced by mining under open-pit final slope is a huge  
9 threat to mine safety. Physical model test is an important method to study mining-induced strata  
10 and surface movement laws. Because of rock joints predominantly control rock mass deformation  
11 and failure, thus physical model test leaving out of consideration of rock joints is difficult to reflect  
12 the influence of rock joints on rock mass deformation. Therefore, this paper presents a three-  
13 dimensional physical model test considering simplified dominant rock joints. This test process  
14 includes the design of testing equipment, the construction of physical model with dominant rock  
15 joint sets, conduction of mining and deformation monitoring. And mining under eastern final slope  
16 of Yanqianshan iron mine was selected as a case to study the behavior of mining-induced strata and  
17 surface movement.

18 **Keywords:** physical model test; rock joint; strata and surface movement; final slope mining; surface  
19 settlement

20

---

21 **1. Introduction**

22 The serious strata and surface movement induced by mining in open-pit final slope would frequently  
23 trigger slope failure and surface subsidence, which would make the mining area into great threaten.  
24 Detailed research on mining-induced strata and surface movement are necessary to prevent and  
25 reduce disasters occurred in mining area. Whereas, there is a great lack of detailed and systematic  
26 studies on strata and surface movement induced by mining under open-pit slope. Methods to study  
27 underground mining-induced rock strata movement are mainly theoretical analysis method,  
28 numerical simulation method, and physical model testing method.

29 The theoretical method simplified the strata as a beam or slab model, and then the simplified  
30 model is analyzed by the mechanical analysis method. The widely used theoretical analysis model to  
31 study this problem are mainly the Pressure-arch Theory. For example, He and Zhang applied the  
32 Discontinuous Deformation Analysis(DDA) in investigating the formation of pressure arch[1]; Wang,  
33 Jing et al. conducted a systematic study on the pressure arch to predict collapse of deep-buried  
34 tunnel[2]. Chen et al. used the Cantilever Hypothesis to analysis the strata movement mechanism  
35 and surface deformation in an iron mine [3]. Tu et al. conducted a research on the gate road system  
36 failure based on the Cantilever Hypothesis [4]. Li et al. studied the static stress within fault-pillars  
37 using the Voussor Beam Theory [5]; Ju and Xu found and defined three kinds of structural model  
38 affected by the key strata's position in super great mining height long wall face [6].

39 The mechanism of mining-induced strata movement can be well understood by the theoretical  
40 analysis method. However, significant inaccuracy is noticeable when simplifying the overlying strata  
41 as beam or slab under complicated geological conditions. With the development of numerical  
42 simulation method and computer technology, numerical simulation method shave been widely used  
43 to study underground mining-induced strata and surface movement. The most common numerical  
44 simulation methods include the Finite Element Method (FEM) and Finite Difference Method (FDM)  
45 based on the continuum mechanics, the Discrete Element Method (DEM) based on the non-

46 continuum mechanics, and method by the combination of FEM and DEM (FEM-DEM) method.  
47 Unver and Yasitli conducted a research on the caving mechanism by FLAC3D [7]; Guo, et al. studied  
48 the strata behavior at long wall panel using COSFLOW software based on the FEM [8]; Wang et al.  
49 simulated the displacement variation, stress and strain of overlying strata and coal seams by ANSYS  
50 software based on the engineering background of working face in Zhao mine [9]; Wang, Kulatilake  
51 et al. simulated a tunnel mining under a high in situ stress condition by using the 3DEC software  
52 package [10]; Gao and Stead studied the mechanism of cutter roof failure by using DEM software  
53 PFC and 3DEC [11]. Xu et al. applied 3DEC to the research of strata and surface movement induced  
54 by mining under final slope [12]; Vyazmensky, Stead et al. analyzed the step-path failure  
55 development induced by block caving in a large open-pit slope by using the FEM/DEM method [13].  
56 Based on numerical simulation the stress, strain and displacement of strata could be conveniently  
57 obtained and analyzed, but on account of the constitutive relation and mechanical parameters of rock  
58 mass are difficult to be defined accurately, hence, significantly different results very likely occur  
59 between the simulation results and actual conditions.

60 Physical model test is also usually adopted to study strata and surface movement caused by  
61 mining. Two-dimensional model with simplified geological condition is usually constructed in  
62 current physical model test, few researchers conduct three-dimensional model test for the difficulty  
63 in model construction, in current physical model test both the two-dimensional and three-  
64 dimensional model can only consider the major structural planes, such as the fault plane and bedding  
65 plane, and the widely-distributed joints in rock mass are always ignored or simplified. While, the  
66 physical model with no consideration of rock joints is difficult to reflect the influence of rock joints  
67 on strata and surface movement [14-18], however, rock joints and their distribution always  
68 dominantly control the rock deformation and strata movement caused by mining.

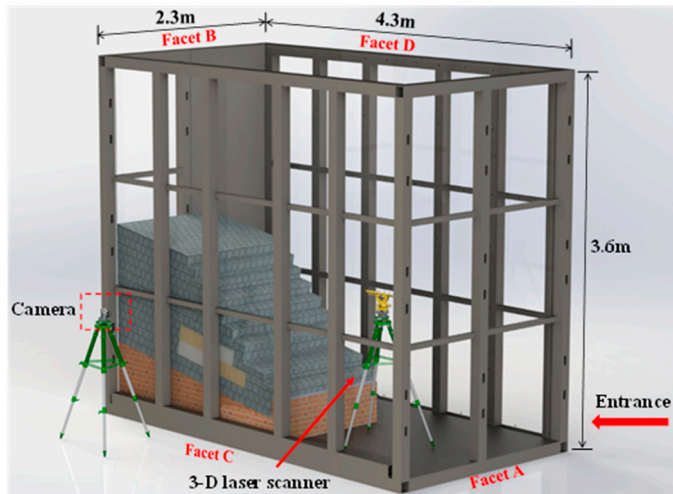
69 In order to reflect the influence of rock joints on strata movement, this paper presents a three-  
70 dimensional physical model test method which can consider the influence of rock joints on strata and  
71 surface movement induced by mining. The proposed method is mainly composed of: the design of  
72 the model box, the construction of physical model with the dominant joints, the mining method, and  
73 the monitoring of model deformation. The eastern final slope in Yanqianshan iron mine, Liaoning,  
74 China was taken as a case to study the strata and surface movement induced by mining. Then the  
75 model test result was analyzed and compared with field observation, and the result indicated that  
76 this method is not only very effective to study mining induced strata and surface movement but also  
77 can reveal the influence of the dominant rock joints on strata and surface movement.

## 78 **2. Materials and Methods**

79 In order to illustrate the testing procedure, the proposed method in this paper was introduced based  
80 on a case study-the underground mining of eastern final slope in Yanqianshan iron mine.

### 81 *2.1. Model box*

82 A model box is indispensable in physical model test and should be constructed according to the  
83 physical dimension of the model and the test requirements. For example, it should have enough  
84 strength and stiffness as well as be convenient for model construction and deformation monitoring  
85 during test. In the case study in this paper, a 4.3 m long, 2.3 m wide, and 3.6 m tall model box (Figure  
86 1) was produced. Facet A of the model box is open to facilitate access by the staff, and facet B is closed.  
87 Facets C and D are made of high-strength plexiglass, through which the deformation of the model  
88 can be monitored.

89  
90**Figure 1.** The model box and monitoring program91 

## 2.2 Model construction

92 Once the prototype was selected the size of test model could be determined based on the  
 93 geometric similar ratio between the prototype and the test model. The similar ratio of the main  
 94 parameters between the prototype and the test model should be determined first based on the  
 95 similarity theory. In order to reflect the main engineering geology and structural characteristics of  
 96 the rock mass, it is necessary to generalize the main distribution characteristics of the actual rock  
 97 joints before construction of the model. To add the dominant joints to the test model, model blocks  
 98 can be used for the model construction. The ore body can be simulated with several sandbags, and  
 99 the step-by-step mining can be conducted by sequent taking the sand out of the sandbag.

100 

### 2.2.1 Production of model blocks

101 The blocks required by a block construction model are made inside the mold. The design of the  
 102 mold needs to be based on the geometry and size of the pre-designed model block, whereas the  
 103 geometry and size of the model block need to be determined based on the distribution of the actual  
 104 joints in the rock. For example, in the case study the distribution of joints in actual rock mass was  
 105 simplified into three sets of equidistant orthorhombic joints, and thus the block required for the  
 106 model construction was designed as a cube.

107 Before making the model blocks, it was necessary to select similar material to produce the model  
 108 blocks. The physical-mechanical parameters of the similar material are defined as the physical-  
 109 mechanical parameters of the actual rock mass divided by the corresponding similar ratios. The  
 110 similar ratios of these parameters are derived based on the similarity theory [19]. In addition,  
 111 materials selected to produce the model blocks should be economic, non-toxic, and easily available.

112 

### 2.2.2 Joint settings

113 In actual rock mass, a large number of joints with various occurrences and sizes frequently  
 114 develop. In a physical model, it is often impossible to simulate a real complex joint system, and  
 115 therefore necessary to simplify the real joint system. Hence, only the dominant joints affecting the  
 116 rock mass structure and strength are taken into account when constructing a physical model. Before  
 117 construction of the model, the dominant joints in actual rock mass are need to be classified into  
 118 several sets according to their occurrences. Each group of joint surfaces is simulated using a number  
 119 of parallel planes, whereas the block geometry for the model construction is determined according  
 120 to the mutual intersection of the actual dominate joints. For example, in the case study, the dominant  
 121 joints were simplified into three sets according the occurrence, and each one is orthogonal to the other  
 122 two. Therefore, the model uses cubes for the block construction. The contact surface between the

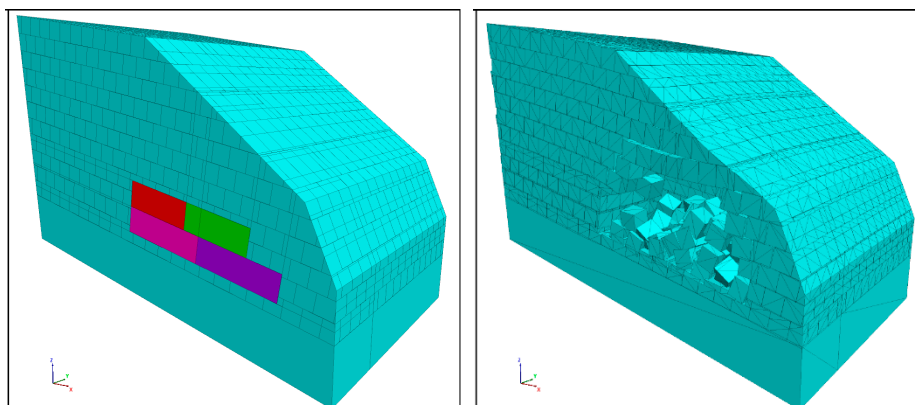
123 blocks is the joint surface, and the side length of the cube is the joint spacing. Before test, the joint  
124 spacing and joint strength should be properly designed.

125 1. Determination of joint spacing.

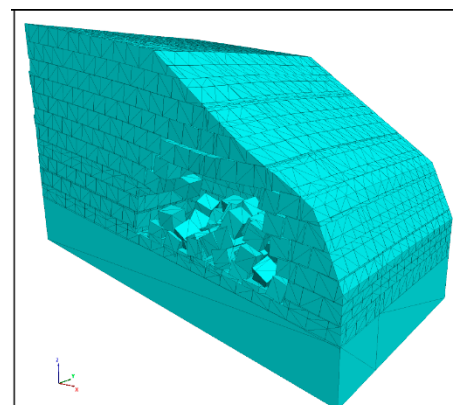
126 According to the similarity theory, the joint spacing should be determined in accordance with  
127 the joint spacing in the actual rock mass divided by a geometric similarity ratio. However, a joint  
128 spacing calculated in this way is occasionally very small, which leads to a small size block required  
129 for the model construction. Small blocks are not only difficult to be made, but also would significantly  
130 increase the number of blocks needed for the model construction. For example, in the case of the  
131 Yanqianshan iron mine, the average joint spacing in real rock mass is about 30-40cm. According to  
132 the geometric similarity ratio of 100:1, the simulated joint spacing is only 3-4mm. When using cube  
133 blocks with a side length of 3-4mm to construct a cube model with a side length of 2m, approximately  
134 290 million test cubes will be required, such a test model cannot be constructed under the existing  
135 test conditions.

136 Therefore, while ensuring that the deformation and destruction characteristics were similar to  
137 the actual situation, joints with as much spacing as possible were added to the model. In this paper,  
138 a Discrete Element Numerical Simulation method was used to determine the appropriate joint  
139 spacing. For example, in the case of open-pit final slope mining at the Yanqianshan iron mine,  
140 different numerical calculation models with different joint spacing were respectively constructed,  
141 and the deformation process of the strata and surface movement was simulated using 3DEC. The  
142 influence of joint spacing on the deformation and failure characteristics of the model was then  
143 analyzed. According to the calculation results, the critical value of joint spacing  $l_{cr}$  can be determined.  
144 When the joint strength spacing is less than  $l_{cr}$ , the influence of joint spacing on the deformation and  
145 failure characteristics of the model will no longer be obvious. Thus,  $l_{cr}$  can be used as the joint spacing  
146 in the model test. In Figure 2, the joint spacing values are from 10cm to 5 cm with a decrement of  
147 0.5cm. Based on the calculation results, the final appropriate joint spacing can be determined as 7.5  
148 cm.

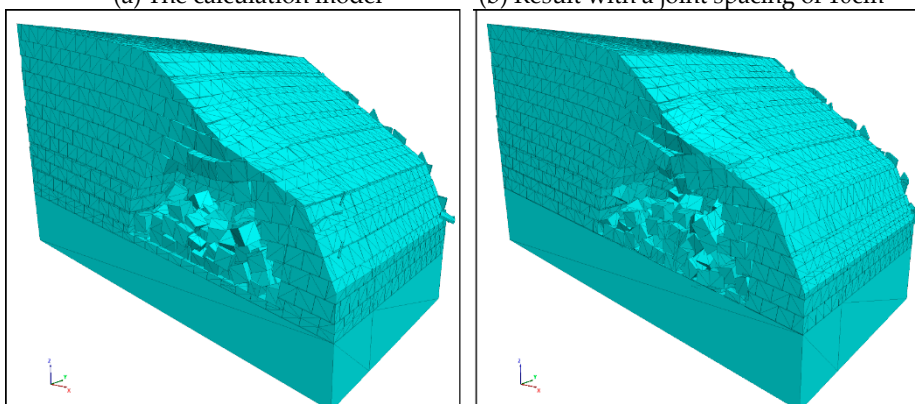
149



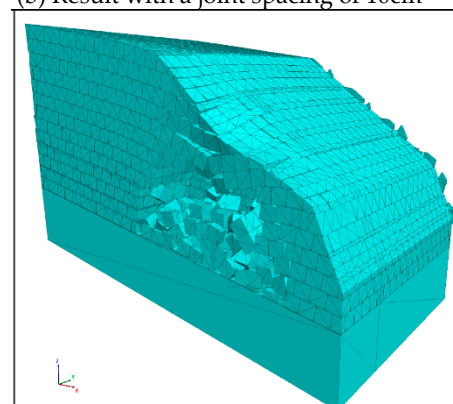
150 151 (a) The calculation model



(b) Result with a joint spacing of 10cm



152 153 (c)Result with a joint spacing of 9 cm



(d) Result with a joint spacing of 8cm

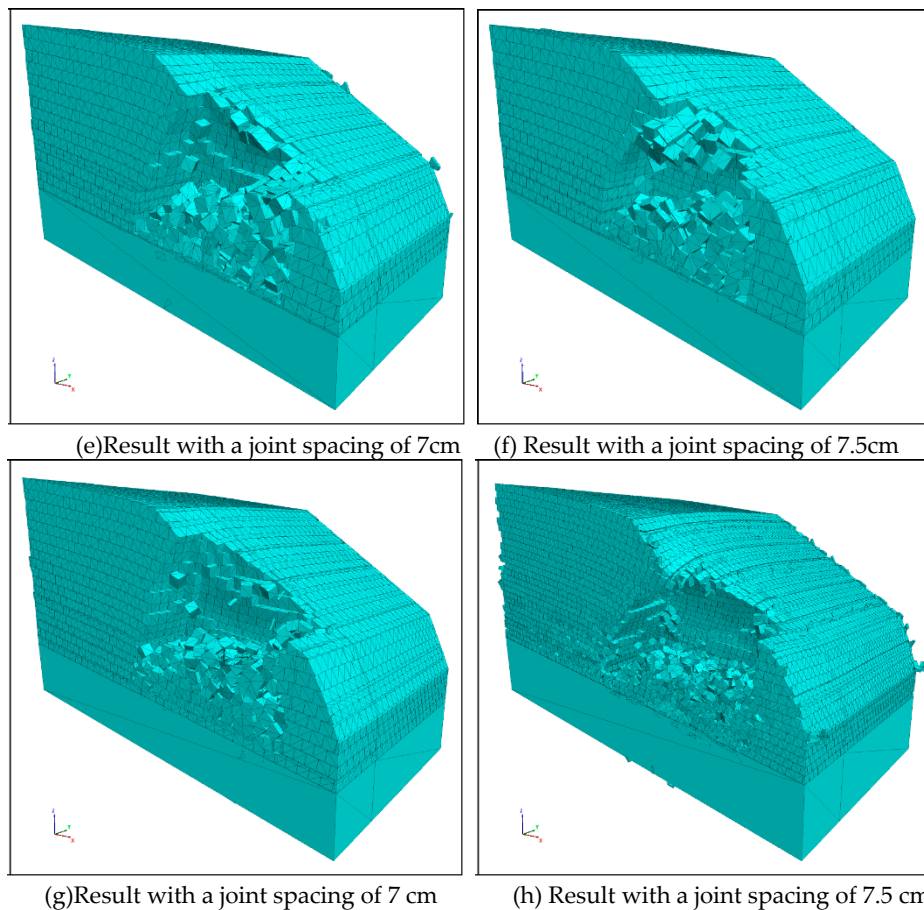


Figure 2. Calculation results with different joint spacing

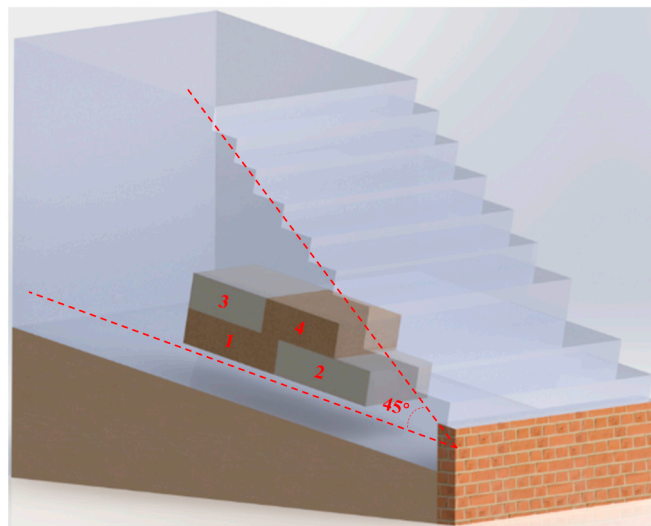
## 2. Determination of joint strength

Joint strength is an important parameter to rock mass deformation and failure, thus in model test the joint strength should be determined according to the real joint strength. The Equivalent Discontinuous Modelling Method of jointed rock mass proposed by Xu and Bayisa is adopted to determine the joint strength, the relationship between joint spacing and joint mechanical parameters was built [20].

In this study the model blocks can be cemented by the adhesive, and the strength of the adhesive applied between the model blocks is the joint strength. The adhesive uses a combination of common building materials such as barite, quartz sand, gypsum, and white latex mixed to a certain proportion, the joint strength is varied while the proportion is different.

## 2.3 Mining design

The design of mining is an important part of a test, and the mining stage and mining way both have a certain impact on the test results. In a 2D model test, embedded test blocks or PVC pipes are often used to simulate an ore body, and in the test described here, the mining was simulated through the extraction of embedded blocks or PVC pipes [22-25]. In this paper, sandbags are used to simulate the ore body, and the sand is removed from the sandbag to model the mining process. This method is closer to an actual mining process. For example, a total of four sandbags were placed for the test described in the case study based on the actual ore body distribution characteristics and the actual mining process, as shown in Figure 3.

178  
179  
180

**Figure 3.** Simulation of ore body and mining process (sandbags #1 to #4 can be removed successively to simulate the mining process)

181 

#### 2.4 Monitoring

182 To avoid failure of the contact measurement method owing to a large local deformation of the  
183 model, non-contact measurement methods can be used to monitor the deformation and failure of the  
184 model, such as 3D laser scanning and digital photogrammetry [18, 22, 23]. The 3D laser scanner and  
185 photogrammeter were used to monitor the surface deformation of the model slope (Figure 1). The  
186 digital point cloud of the slope after each step of mining can be obtained by scanning the slope  
187 surface, and the displacement of the slope can be calculated. In the case study as shown in Figure 2,  
188 the C-facet of the model was in fact a vertical section along the center of the veins, and the strata and  
189 surface movement could be observed in this section. Therefore, for this study, we drew a series of  
190 identification points on a block near the glass side, and used a photogrammeter to obtain the initial  
191 state of the model and the location of each identification point during the mining process. Based on  
192 the results of each measurement, the displacement vector of the lateral block was calculated, and the  
193 behaviors of strata and surface movement were obtained.

194 

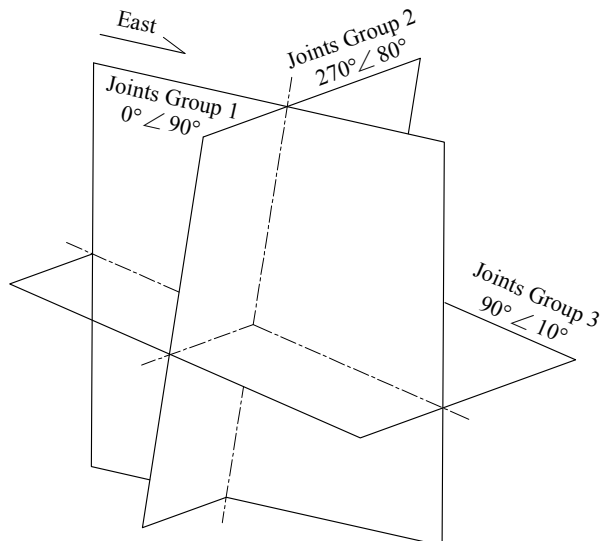
### 3. Case study

195 

#### 3.1. Geological background

196 The Yanqianshan iron mine is located in Anshan City, Liaoning Province, China. The basic  
197 structural pattern of the mining area is a steep monoclinic structure trending toward a direction of  
198  $270^\circ\text{--}300^\circ$ , with a dip in direction toward the northeast or southeast, and a dip angle of  $70^\circ\text{--}88^\circ$ ; that  
199 is, the structure is partially upright. In the area of the eastern final slope, the iron ore body is located  
200 in the middle, strikes almost east-east, and dips to the northeast at approximately  $70^\circ$ . The ore body  
201 of the eastern final slope has a length of 300m~550m and an average thickness of 80m. The eastern  
202 final slope is located east of the XIV prospecting line until the open-air area, and has relatively  
203 developed fissures. Three sets of mutually intersecting dominant joints are developed in the rock,  
204 with one of the sets being a strata layer and other two sets intersecting this layer at a large angle while  
205 also intersecting each other. And to facilitate the modeling, in this study, the distribution of joints in  
206 the model is generalized into an orthogonal intersection, see in Figure4. The typical rock types and  
207 physical-mechanical parameters of rock mass in Yanqianshan iron mine are listed in Table 1.

208



209

210

**Figure 4.** The simplified three dominant sets of joints in test model.

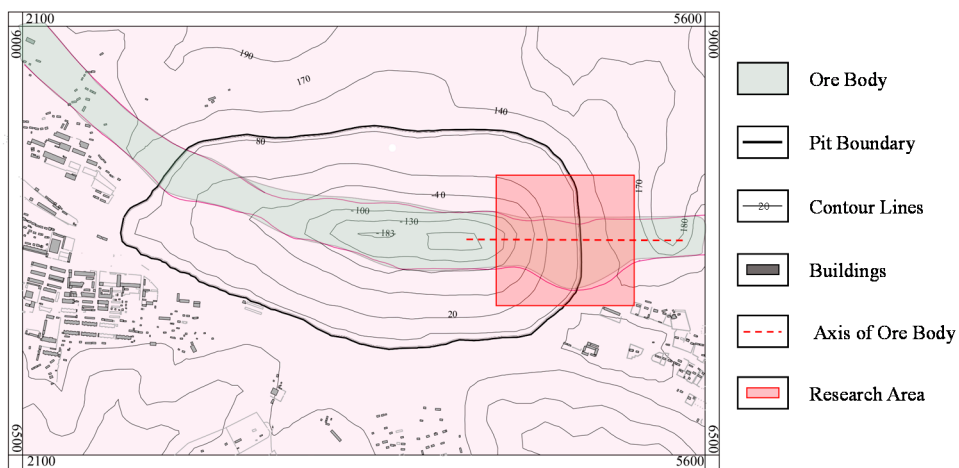
211

**Table 1.** Physical-mechanical parameters of rock masses in Yanqianshan iron mine

Rock mass	Compressive strength(MPa)	Deformation modulus(GPa)	Cohesion(MPa)	Internal friction angle(°)
Mixed rock	164.34	3~5	40~50	38~40
Diorite	181.47	2	55~60	40~42
Carbonaceous phyllite	44.52	1.5	35~38	35~38
Chlorite quartz schist	98.56	1.5~2	40~45	38~40

212  
213  
214

To visually observe the deformation of the surrounding rock in the mined-out area, we divided the eastern final slope into two parts along the axis of the iron vein, and selected one as the simulated model. The red shaded area in Figure 5 was selected as the prototype.



215

216

**Figure 5.** The eastern final slope to be studied is in red shade.

217

### 3.2. Model block production

218 For a physical model test, the geometric and material similarities of the model need to be  
 219 controlled based on the similarity theory to reflect the deformation and failure of the rock mass under  
 220 real conditions. The similarity ratio of controlling parameters are shown in Table 2. The joint spacing  
 221 of the model was set to 7.5 cm, and three sets of mutually orthogonal joints were added in the model.  
 222 Thus, cube blocks with a side length of 7.5 cm were produced using a similar material, and then used  
 223 to construct the test model. For this study, a material similar to mixed rock found as the major rock  
 224 type in the Yanqianshan iron mine was used to develop the blocks applied during the test. Based on  
 225 the principles of economy, non-toxicity, and availability, the mixture of cement, quartz sand, barite,  
 226 iron powder, gypsum, and water were selected to produce the blocks, the final mass proportion of  
 227 the similar material used was determined through orthogonal tests and mathematical analysis. The  
 228 final mass proportion and mechanical parameters of the similar material are shown in Tables 3 and  
 229 4. Between the blocks, an adhesive made of barite, quartz sand, gypsum, and white latex was applied  
 230 to keep the blocks cemented. The adhesive between the blocks was made of a mixture of barite, quartz  
 231 sand, gypsum, and white latex with a certain proportion. The proportions of these materials are  
 232 shown in Table 5, and the strength of the adhesive is the joint strength, as shown in Table 6.

233 **Table 2.** Similarity ratios of the main controlling parameters

Parameters	Similarity Relationship	Similarity ratio
Geometry( $C_L$ )	— —	200
Bulk Density( $C_r$ )	— —	1
Stress( $C_\epsilon$ )	— —	1
Poisson's Ratio( $C_\mu$ )	— —	1
Friction Angle( $C_\varphi$ )	— —	1
Strain( $C_\sigma$ )	$C_\sigma = C_\gamma \times C_L$	200
Elastic Modulus	$C_E = \frac{C_\sigma}{C_\epsilon}$	200

234 **Table 3.** The mass proportion of similar material

Cement	Quartz sand	Barite	Iron powder	Gypsum	Water
1	28	28	6.67	3	7.07

235 **Table 4.** The properties of similar material used in this paper

Density (g/cm <sup>3</sup> )	Uniaxial compressive strength (MPa)	Deformation modulus (MPa)	Cohesive (MPa)	Friction angle (°)
2.56	0.80	200.61	0.1735	38.94

236 The adhesive between the blocks was made of a mixture of barite, quartz sand, gypsum, and  
 237 white latex. The mass proportions of these materials are shown in Table 5, and the strength of the  
 238 joints in test model is shown in Table 6.

239 **Table 5.** The mass proportion of adhesive

Barite	Quartz sand	Gypsum	White latex
3.5	4.8	0.9	1

240 **Table 6.** The mechanical property of simulated joint

Cohesive (MPa)	Friction angle (°)	Tension strength (MPa)
0.164	20.45	0.00698

## 241 3.3. Model generalization

242 The generalization of the model was carried out according to the geological and geometric  
 243 characteristics of the eastern final slope at the Yanqianshan iron mine. The study area was scaled  
 244 down according to a geometric similarity ratio of 200:1. The resulting test model has a length of 2.3  
 245 m, width of 1.2 m and height of 2.0 m. The slope is inclined toward the eastern direction, and thus  
 246 the three simplified sets of joints in the model are  $90^\circ \angle 20^\circ$ ,  $0^\circ \angle 90^\circ$ , and  $270^\circ \angle 70^\circ$  (Figure 4),  
 247 respectively. The ore body in test model is approximately 0.75 m from the top of the slope, with a  
 248 length of approximately 1m, a width of approximately 0.4 m, and a thickness of approximately 0.2 m  
 249 (Figure 6). The mining was designed to conduct at two levels, each of which having two steps. That  
 250 is, during the test process, sandbags #1, #2, #3, and #4, shown in Figure 7 were “mined out”  
 251 successively.



252

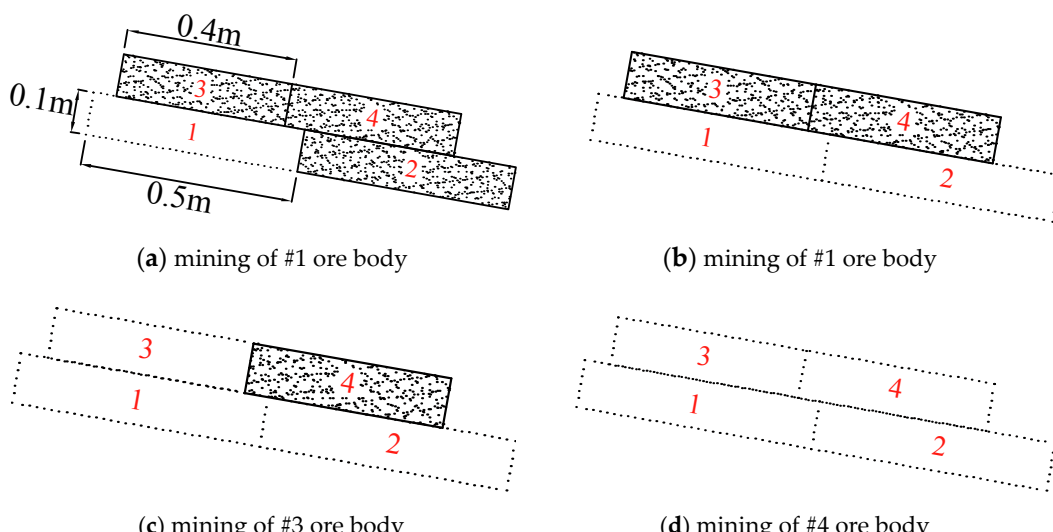
253

(a) The side view of

254

(b) The front view

Figure 6. The side view and front view of the completed model



255

256

(a) mining of #1 ore body

(b) mining of #1 ore body

(c) mining of #3 ore body

(d) mining of #4 ore body

257

258

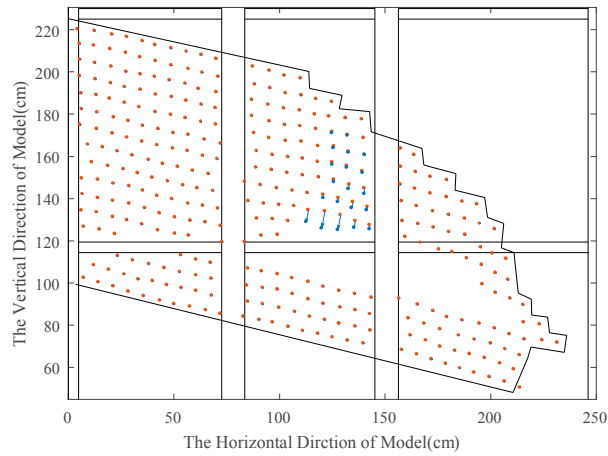
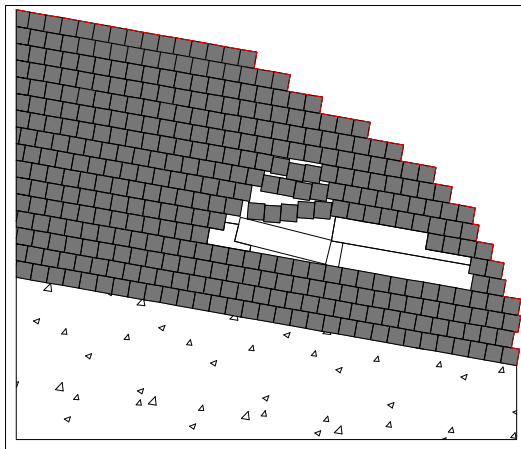
259 Figure 7. Illustration of the mining process

260 3.4. Testing process and results

261 3.4.1. Testing process

262 The test process involves the mining of ore bodies #1~#4. The model deformation after each step  
263 of mining is shown in figure 8~figure11.

264 Step1: Mining of ore body #1 (Figure 8(a)). After mining ore body #1, the model mainly had local  
265 deformations with clear vertical zoning characteristics. The first layer of blocks on the roof of the  
266 mined-out area collapsed and fell off, forming a local collapse zone. Then strata overlying this layer  
267 underwent a significant downward deflection, forming a deflection zone, which caused a certain  
268 degree of open deformation of the overlaying strata along the flat and steep joints, thereby forming  
269 a fractured zone (Figure 8(c)). From above the fractured zone to the slope surface, no significant  
270 deformation and failures occurred. And the displacement in figure 8(b) also indicated that the  
271 direction of strata movement was vertical downward to the mined-out area, and the maximum  
272 displacement appeared at the roof of the mined out area.



273

274

275

(a) Sketch of test model

(b) Displacement vector



276

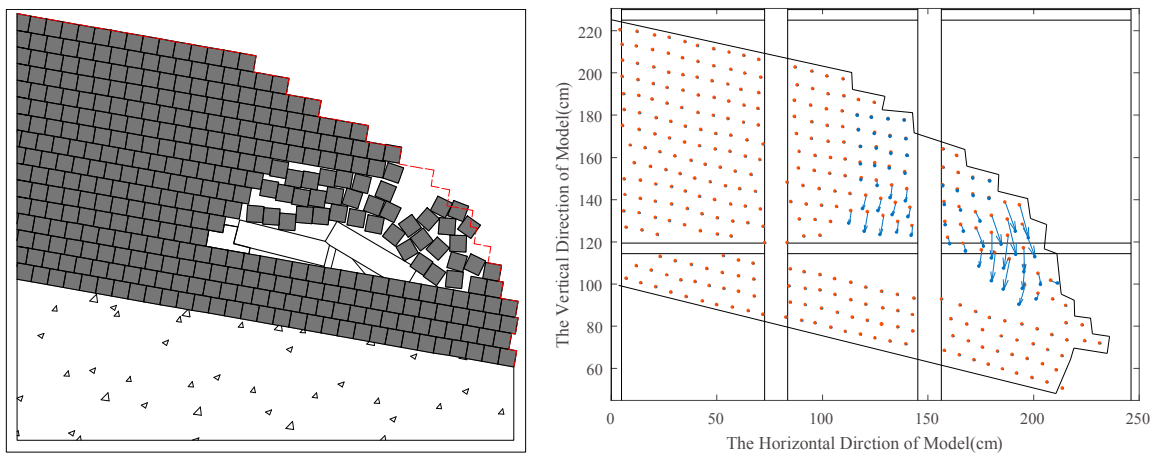
277

(c) Deformation of test model after mining #1 ore body

278

Figure 8. Deformation occurred after mining #1 ore body

279 Step 2: Mining of ore body #2 (Figure 9(a)). After mining ore body #2, the strata further deformed  
 280 along the already opened joint surface, and significant dislocation of model blocks occurred along  
 281 the steep joint surface (figure 9(a)). The range of mined-out area developed, and the strata above the  
 282 mined-out area collapsed vertically. From above the collapse zone to the slope surface, as the  
 283 downward deflection further developed, an obvious subsidence pit on the slope surface was  
 284 appeared, as shown in Figure 9(c). The strata on the slope surface above the mined-out area  
 285 underwent significant deflection, opening mainly along the steep joint surface, and the model blocks  
 286 experienced an intensive disturbance, as shown in figure 9(a). after mining of ore body #2,  
 287 displacement of the test model was enlarged generally, the maximum displacement appeared above  
 288 ore body #2, and the vector showed that surface blocks were mainly moved along the slope surface,  
 289 blocks on the roof of the mined-out area were mainly moved vertical downward(9(b)).



290

291

(a) Sketch of test model

(b) Displacement vector

292  
293

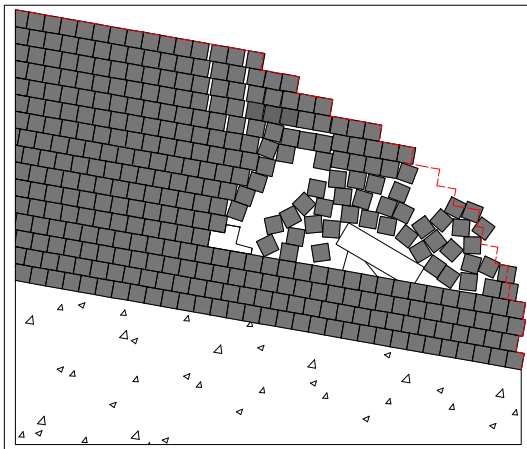
(c) Deformation of test model after mining #2 ore body

294

**Figure 9.** Deformation occurred after mining #2 ore body

295 Step3: Mining of ore body #3 (figure 10(a)). After mining ore body #3, all blocks in the fractured  
 296 zone collapsed, forming a large caving zone, as shown in Figure 10(c). The surrounding rock in the  
 297 mined-out area experienced a topple avalanche toward the surface, however, the strata on top of the  
 298 mined-out area first underwent a vertical wide-range collapse. Obvious continuous deformation  
 299 appeared. Displacement vector in figure 10(b) illustrated that while the mined-out are enlarged the  
 300 surrounding rock mass were prone to the move toward the mined-out area. The range of slope  
 301 surface subsidence further expanded. Toppling avalanche toward the mined-out area occurred in the  
 302 surrounding rock mass, and as the rock mass deformation further developed, strata right above the

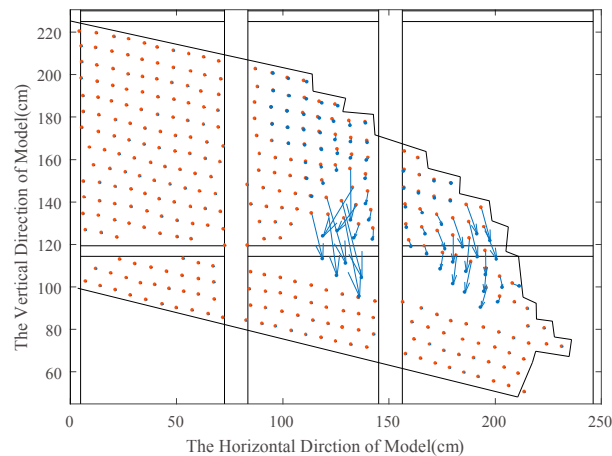
303 #3 ore body extensively fractured, and continuous deformation developed from the fractured zone  
 304 to the slope surface. Traces of slide deformation were observed right above #2 ore body. Joint surfaces  
 305 in fractured zone were further opened. The slope surface right above #2 ore body mainly experienced  
 306 subsidence deformation, and significant slipping deformation occurred on the lower slope surface.



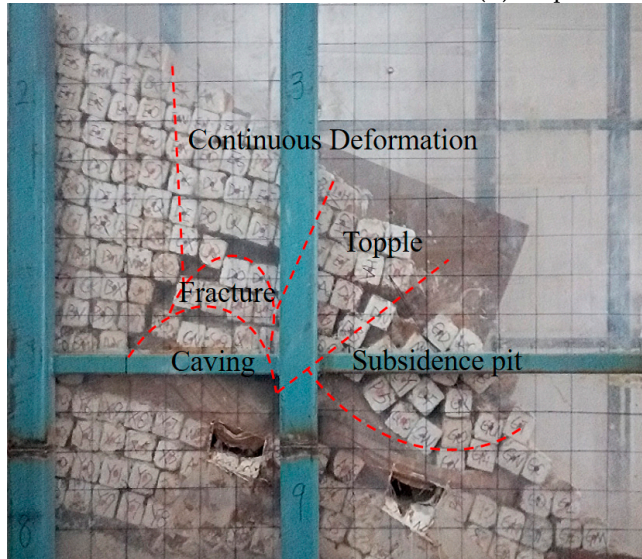
307

308

(a) Sketch of test model



(b) Displacement vector

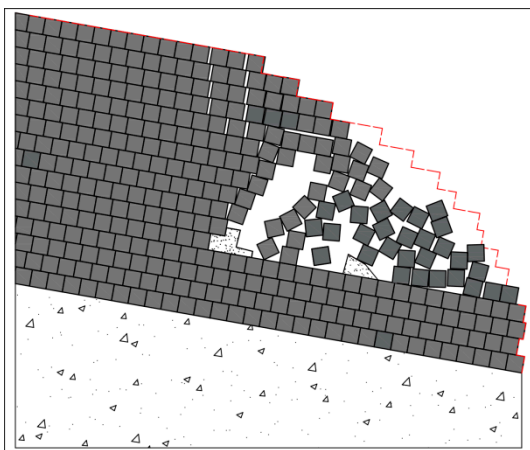
309  
310

(c) Deformation of test model after mining #3 ore body

311

Figure 10. Deformation occurred after mining #3 ore body

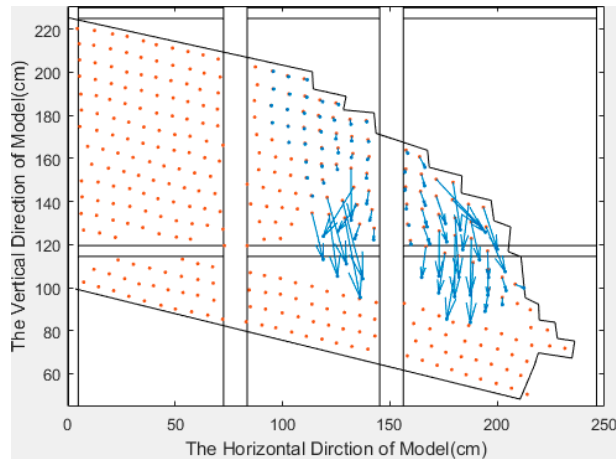
312 Step4: Mining of ore body #4 (Figure 11(a)). The strata on roof of the mined-out area collapsed  
 313 entirely. The surrounding rock of the mined-out area underwent a toppling avalanche toward the  
 314 mined-out area, and eventually accumulated inside the mined-out area. The accumulated blocks  
 315 resisted further toppling collapse of the surrounding rock. On the boundary of the mined-out area,  
 316 significant shear dislocation deformation could be observed, as shown in the detailed view in Figure  
 317 11(c). The range of the subsidence pit on the slope surface continued to develop. Model blocks near  
 318 the subsidence pit experienced intensive disturbance and started to slip along the bedding surface.  
 319 The displacement vector in figure 11(b) showed that several blocks on slope surface avalanched, the  
 320 surrounding blocks of the mined-out area mainly moved toward it, and the surface blocks mainly  
 321 underwent subsidence and local sliding along the bedding surface.



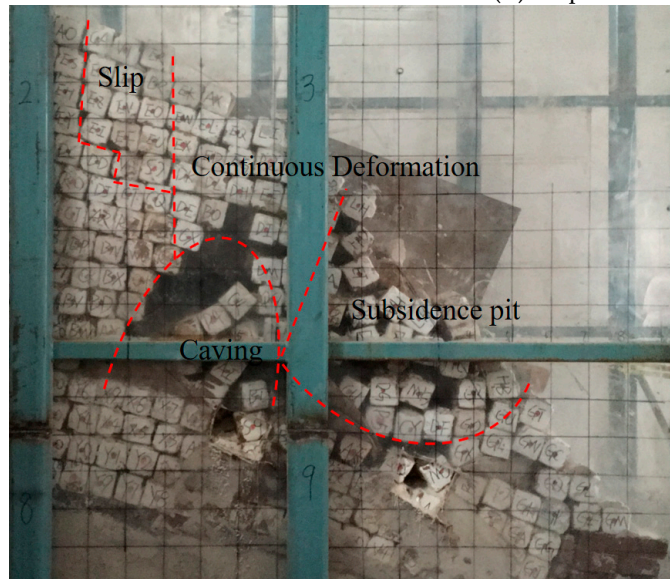
322

323

(a) Sketch of test model



(b) Displacement vector



324

325

(c) Deformation of test model after mining #4 ore body

326

Figure 11. Deformation occurred after mining #4 ore body

## 327 3.4.2 Characteristics of mining-induced strata and surface movement

328 The upper rock mass in the mined-out area is dominated by "well-shaped" collapse. Continuous  
 329 deformation occurred on the overlying slope surface of the ore body and formed a subsidence pit,  
 330 the boundary of which is fundamentally a steep joint surface. Displacement vector map show that  
 331 the collapse pit has steep and straight boundaries, yielding a clear well shape of the cross section. The  
 332 above test phenomena and monitoring results show that subsidence occurred in rocks with steep and  
 333 dense joints differs from the "trumpet-shaped" subsidence in a homogeneous rock mass.

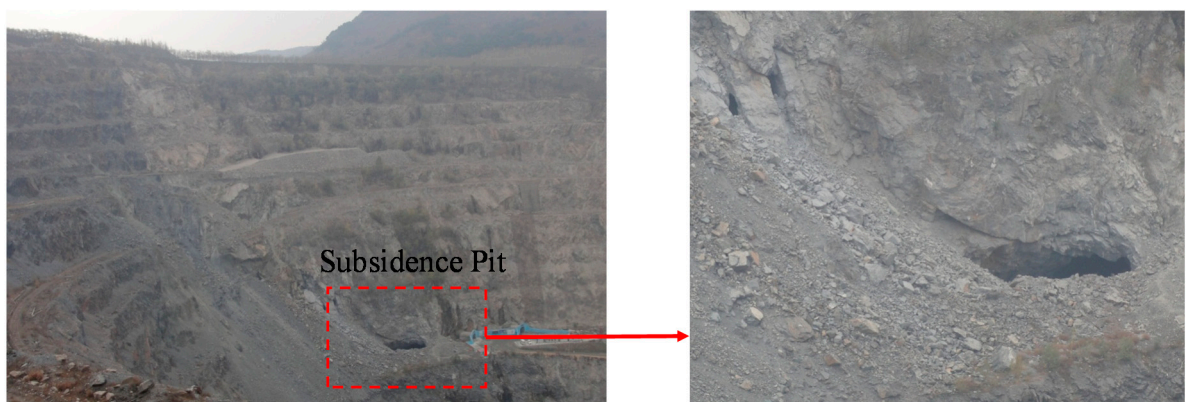
334 At the beginning of mining, the deformation of the rock mass presented a typical vertical zoning  
 335 characteristic. From the roof of the mined-out area to the slope surface, a collapse zone (complete  
 336 collapse of blocks), fractured zone, and deflection zone occurred (figure 8). Meanwhile, the model  
 337 blocks that had collapsed and accumulated in the mined-out area could prevent further deformation  
 338 of the surrounding rock. As the mining progressed, the mined-out area expanded, and the strata  
 339 deformation in the fracture zone further increased until a collapse occurred, and the fractured zone  
 340 transforms into the collapse zone. Due to the influence of the blocks accumulated in the mined-out  
 341 area, the overlying and sloping strata deformation in the mined-out area also exhibited significant  
 342 zoning characteristics in the horizontal direction. From the back edge of the slope to the end of the  
 343 slope, the following occurred: 1. at the top-left of the mined-out area, model blocks mainly slid along

344 the strata layer, and the back edge of the slide area and the middle strata opened substantially along  
345 the steep joint surface. 2. In the area directly above the mined-out area, the model blocks mainly  
346 subsidized vertically along the steep joint surface toward the mined-out area, the steep joint surface  
347 on the boundary of the area was substantially opened, and the model blocks at the boundary  
348 underwent significant dislocation. 3. Finally, at the top-right of the mined-out area, model blocks in  
349 the front of the mined-out area, particularly those on the slope surface, experienced a sliding  
350 avalanche and eventually accumulated along the slope surface under the subsidence pit, forming an  
351 accumulation zone (figure 11).

352 **4 Discussion**

353 *4.1 The cause of "well-shaped" collapse*

354 Rock deformation and failure is predominantly controlled by the dominant joints, deformation  
355 always developed along dominate joint surfaces with relative weak strength [12, 25]. Whereas, it is  
356 one of the main challenges to reflect the joints' influence on strata deformation. Therefore, the 3D  
357 physical model test with consideration of dominant rock joints is presented. In this paper the test  
358 method was adopted to study the strata and surface movement induced by mining under the eastern  
359 final slope in Yanqianshan iron mine, and the test results revealed that the "well-shaped" collapse  
360 mainly occurred in rock mass with steep dominant joints, which is strikingly different with the  
361 "trumpet-shaped" collapse occurred in rock mass without dominant joints [22, 23, 26, 27]. During the  
362 mining, the surrounding rock mass subjected unloading resulted from mining resulted in rock mass  
363 deformation toward the mined-out area, thus rock mass on side wall of the mined-out area deformed  
364 to the mined-out, due to the existence of steep joint surface, toppling avalanche of blocks occurred  
365 along the joints surfaces. Whereas rock mass on the roof of mined-out area collapsed and the  
366 overlying rock mass underwent downward deflection due to the mining-induced unloading and the  
367 gravity of overlying strata. Thus the "well -shaped" collapse occurred, and the corresponding surface  
368 subsidence occurred at slope surface, the failure is identical with the field observation in Yanqianshan  
369 iron mine (figure 12). Whereas in homogeneous rock mass the "trumpet-shaped" or "funnel-shaped"  
370 collapse mainly occur, which means intensive subsidence just occurred in a shallow depth from the  
371 slope surface and strata movement is markedly mitigated from the surface to the mined-out area.  
372 whereas, in rock mass with steep dominant joints, almost strata from the surface to the mined-out  
373 area collapsed, thus the steep joints controls the depth and direction of strata and surface movement.



374

375 **Figure 12.** Subsidence pit observed at eastern final slope in Yanqianshan

376 The mined-out area-directional movement was the main deformation in the two sides of mined-  
377 out area. Following steep joints opened under unloading effect in the above mentioned process, the  
378 strata avalanched and toppled in the two sides of mined-out area. After mining ore body #4, the  
379 surrounding strata were seriously disturbed with some joint surfaces opened, and strata dislocation

380 etc. Further deformation of surrounding rock mass was prevented by the blocks accumulated in the  
381 mined-out area.

382 *4.2 Discussion on the experiment method*

383 As an important research method, the physical model test has difficulties and limitations in  
384 quantitative research, however, this method can directly reflect the real process of strata movement  
385 in natural condition. The whole deformation process obtained from the test can provide an important  
386 reference to quantitative research. The 2-D physical model is mainly adopted with the simplified  
387 geological conditions, without considering the important influence of widely-spread joints in the real  
388 rock mass. The joints' absence in the physical model would lead to large differences between the  
389 experiment result and field observation, which is one of the challenges in physical model test method  
390 presently. In order to solve this problem, model blocks made of similarity materials were used to  
391 construct the test model, and the joints were simulated by the interfaces between the blocks. In order  
392 to satisfy the real joint strength, adhesive made by similar materials with certain proportion was filled  
393 in the interfaces, thus the joint strength in the test model could be determined. Both the production  
394 of the model blocks and the construction of the test model based on the similarity theory, all the  
395 materials used to produce the model blocks were inexpensive, nontoxic and available.

396 The phenomena of model test should well reflect the real deformation of geological body. The  
397 mechanism of strata and surface movement obtained is well agreement with the field observation  
398 and numerical simulation results. They are complement and support each other. The experiment  
399 results are verified by the field observation in the Yanqianshan iron mine, especially the mechanism  
400 of strata and surface movement was valuable to analyze the mining-induced failure at the eastern  
401 final slope in the Yanqianshan iron mine. For example, deformation and failure of rock mass at  
402 eastern final slope are: In 2014, the overlying strata has no large-scale deformation after mining; in  
403 2015, the "well-shaped" subsidence pit has occurred, and the rock blocks at the back edge of the slope  
404 fell down into the pit. The transportation road was destroyed by the subsidence pit. Then the  
405 subsidence pit were further developed. At the beginning of mining, the strata presented a vertical-  
406 directional subsidence deformation, which caused by mining-induced unloading and the gravity of  
407 overlying strata. The "well-shaped" subsidence pit with the boundary along the steep joint surfaces  
408 reflects the influence of dominant joints on the strata movement. The experiment reproduced the real  
409 strata movement process, and revealed the controlling effect of dominant joints on strata movement.  
410 The 3D physical model test method proposed in this paper provides an effective method to study  
411 mining-induced strata and surface movement in jointed rock mass.

412 **5 Conclusions**

413 In this paper, a 3D physical model test method was proposed that incorporates simplified joints  
414 in the model. The method generalizes the dominant joints based on their real distribution in rock  
415 mass, and then builds the model through a block construction. The interfaces between the blocks act  
416 as the joint surface, the joint strength is determined based on the Equivalent Discontinuous Modeling  
417 Method of jointed rock mass. This testing method can theoretically be used to construct model with  
418 any joint distribution and strength. The test process mainly includes the model box design and  
419 production, generalization and construction of a 3D physical model with dominant joints, mining  
420 design, and monitoring. A numerical calculation method is adopted to calculate the effects of  
421 different joint spacing on the test results, and the appropriate joint spacing is determined based on  
422 the calculation results.

423 Mining under the eastern final slope at the Yanqianshan iron mine was taken as an case study in  
424 this paper and the test results indicate that the mining-induced "well-shaped" collapse would mainly  
425 occur in rock mass with steep dominant joints. At the early mining stage, the strata and surface

426 movement has an obvious vertical zoning characteristic, whereas it exhibits an apparent horizontal  
427 zoning as the mining proceeds until the end.

428 The test phenomena described in this paper are consistent with the actual deformation and  
429 failure of the eastern final slope, and reflect the effects of the dominant joints on mining-induced  
430 strata and surface movement. Thus the test method proposed herein can intuitively reflect the entire  
431 process of mining-induced strata and surface movement at the microscopic scale.

432 **Acknowledgements:** Thanks for the editor and the reviewers for their helpful comments, which greatly  
433 improved the quality of the manuscript. This research is a part of a project sponsored by the National Natural  
434 Science Foundation of China, project under grants of 41772326 and 41302234. The Fundamental Research Funds  
435 for the Central Universities (2652016105).

436 **Supplementary Materials:** The following are available online at [www.mdpi.com/link](http://www.mdpi.com/link), Figure S1: title, Table S1:  
437 title, Video S1: title.

438 **Author Contributions:** "Kunpeng Gao, Guoxiang Yang and Nengxiong Xu conceived and designed the  
439 experiments; Kunpeng Gao performed the experiments; Kunpeng Gao analyzed the data; Kunpeng Gao and  
440 Guoxiang Yang wrote the paper."

#### 441 References

- 442 1. He, L.; Q. B. Zhang. Numerical investigation of arching mechanism to underground mining in jointed rock  
443 mass. *Tunneling and Underground Space Technology* **2005**, *50*: 54-67.
- 444 2. Wang, Y., H. Jing, Q. Zhang, N. Luo and X. Yin. Prediction of Collapse Scope of Deep-Buried Tunnels Using  
445 Pressure Arch Theory. *Mathematical Problems in Engineering* **2016**, *1-10*.
- 446 3. Cheng, G., C. Chen, T. Ma, H. Liu and C. Tang. A Case Study on the Strata Movement Mechanism and  
447 Surface Deformation Regulation in Underground Iron Mine. *Rock Mechanics and Rock Engineering* **2016**,  
448 *50*(4): 1011-1032.
- 449 4. Bai, Q., S. Tu, F. Wang and C. Zhang. Field and numerical investigations of gateroad system failure induced  
450 by hard roofs in a longwall top coal caving face. *International Journal of Coal Geology* **2017**, *173*: 176-199.
- 451 5. Li, Z.-l., L.-m. Dou, W. Cai, G.-f. Wang, Y.-l. Ding and Y. Kong. Mechanical Analysis of Static Stress With  
452 in Fault-Pillars Based on a Voussoir Beam Structure. *Rock Mechanics and Rock Engineering* **2015**, *49*(3): 1097-  
453 1105.
- 454 6. Ju, J. and J. Xu. Structural characteristics of key strata and strata behavior of a fully mechanized longwall  
455 face with 7.0m height chocks. *International Journal of Rock Mechanics and Mining Sciences* **2013**, *58*: 46-54.
- 456 7. Unver, B. and N. E. Yasitli. Modelling of strata movement with a special reference to caving mechanism in  
457 thick seam coal mining. *International Journal of Coal Geology* **2016**, *66*(4): 227-252.
- 458 8. Guo, H., L. Yuan, B. Shen, Q. Qu and J. Xue. Mining-induced strata stress changes, fractures and gas flow  
459 dynamics in multi-seam longwall mining. *International Journal of Rock Mechanics and Mining Sciences* **2012**,  
460 *54*: 129-139.
- 461 9. Ye, Q., W.-j. Wang, G. Wang and Z.-z. Jia. Numerical simulation on tendency mining fracture evolution  
462 characteristics of overlying strata and coal seams above working face with large inclination angle and  
463 mining depth. *Arabian Journal of Geosciences* **2017**, *10*(4): 82.
- 464 10. Wang, X., P. H. S. W. Kulatilake and W.-d. Song. Stability investigations around a mine tunnel through  
465 three-dimensional discontinuum and continuum stress analyses. *Tunneling and Underground Space  
466 Technology* **2012**, *32*: 98-112.
- 467 11. Gao, F. and D. Stead. Discrete element modelling of cutter roof failure in coal mine roadways. *International  
468 Journal of Coal Geology* **2013**, *116-117*: 158-171.
- 469 12. Xu, N., J. Zhang, H. Tian, G. Mei and Q. Ge. Discrete element modeling of strata and surface movement  
470 induced by mining under open-pit final slope. *International Journal of Rock Mechanics and Mining Sciences*  
471 **2016**, *88*: 61-76.
- 472 13. Vyazmensky, A., D. Stead, D. Elmo and A. Moss. Numerical Analysis of Block Caving-Induced Instability  
473 in Large Open Pit Slopes: A Finite Element/Discrete Element Approach. *Rock Mechanics and Rock  
474 Engineering* **2009**, *43*(1): 21-39.

475 14. Ren, W., C. Guo, Z. Peng and Y. Wang. Model experimental research on deformation and subsidence  
476 characteristics of ground and wall rock due to mining under thick overlying terrane. *International Journal of*  
477 *Rock Mechanics and Mining Sciences* 2010, 47(4): 614-624.

478 15. Weishen, Z., L. Yong, L. Shucui, W. Shugang and Z. Qianbing. Quasi-three-dimensional physical model  
479 tests on a cavern complex under high in-situ stresses. *International Journal of Rock Mechanics and Mining*  
480 *Sciences* 2011, 48(2): 199-209.

481 16. Li, S. C., Q. Wang, H. T. Wang, B. Jiang, D. C. Wang, B. Zhang, Y. Li and G. Q. Ruan. Model test study on  
482 surrounding rock deformation and failure mechanisms of deep roadways with thick top coal. *Tunnelling*  
483 *and Underground Space Technology* 2015, 47: 52-63.

484 17. Fang, Y., C. Xu, G. Cui and B. Kenneally. Scale model test of highway tunnel construction underlying  
485 mined-out thin coal seam. *Tunnelling and Underground Space Technology* 2016, 56: 105-116.

486 18. Ju, M., X. Li, Q. Yao, S. Liu, S. Liang and X. Wang. Effect of sand grain size on simulated mining-induced  
487 overburden failure in physical model tests. *Engineering Geology* 2017, 226: 93-10.

488 19. Luo, X.Q.; Ge X. R. Theory and application of model test on landslide. China Water Power Press 2008.

489 20. Bayisa Regassaa, b, Nengxiong Xu, Gang Mei. An Equivalent Discontinuous Modeling Method of Jointed  
490 Rock Masses for DEM Simulation of Mining-induced Rock Movements. *Engineering Geology*  
491 2017(submitted)

492 21. Huayang, D., L. Xugang, L. Jiyan, L. Yixin, Z. Yameng, D. Weinan and C. Yinfei. Model study of  
493 deformation induced by fully mechanized caving below a thick loess layer. *International Journal of Rock*  
494 *Mechanics and Mining Sciences* 2010, 47(6): 1027-1033.

495 22. Ghabraie, B., G. Ren, J. Smith and L. Holden. Application of 3D laser scanner, optical transducers and  
496 digital image processing techniques in physical modelling of mining-related strata movement. *International*  
497 *Journal of Rock Mechanics and Mining Sciences* 2015, 80: 219-230.

498 23. Ghabraie, B., G. Ren and J. V. Smith. Characterising the multi-seam subsidence due to varying mining  
499 configuration, insights from physical modelling. *International Journal of Rock Mechanics and Mining Sciences*  
500 2017, 93: 269-279.

501 24. Xu, Y., K. Wu, L. Li, D. Zhou and Z. Hu. Ground cracks development and characteristics of strata  
502 movement under fast mining: a case study at Bulianta coal mine, China. *Bulletin of Engineering Geology and*  
503 *the Environment* 2017, 1-16.

504 25. Sun, G. *Rockmass Structural Mechanism* 1988, Beijing, China : Science Press.

505 26. Guo, Q., G. Guo, X. Lv, W. Zhang, Y. Lin and S. Qin. Strata movement and surface subsidence prediction  
506 model of dense solid backfilling mining. *Environmental Earth Sciences* 2016, 75(21).

507 27. Xu, D., S. Peng, S. Xiang and Y. He. A Novel Caving Model of Overburden Strata Movement Induced by  
508 Coal Mining. *Energies* 2017, 10(4): 476.